Journal of Cleaner Production 313 (2021) 127758

Contents lists available at ScienceDirect

Journal of Cleaner Production

journal homepage: www.elsevier.com/locate/jclepro

Degradation of rhodamine B in water by ultrasound-assisted TiO_2 photocatalysis

Dong Xu [a,1], Hailing Ma [b,*,1]

[a] College of Geomatics and Municipal Engineering, Zhejiang University of Water Resources and Electric Power, Hangzhou, 310018, China
[b] Institute of Mechanics, Chinese Academy of Sciences, Beijing, 100190, PR China

ARTICLE INFO

Editor: Zhen Leng

Keywords:
Ultrasound
Rhodamine B
Degradation
Photocatalysis

ABSTRACT

Rhodamine B is widely used in the dyeing of paints, acrylic and other fabrics as well as biological products. It is highly toxic to organisms when directly discharged into water. To this end, in this paper, degradation of Rhodamine B in water by ultrasound-assisted TiO_2 photocatalysis was investigated. The effects of various factors, such as the amount of catalyst, the speed of mechanical stirring, the frequency of ultrasonic vibration, the ultrasonic output power, the initial pH value of the reaction solution, the initial concentration of Rhodamine B, the introduced air, and physical adsorption, etc., on the degradation of Rhodamine B in wastewater were studied, and the optimal degradation conditions were obtained: rotational speed, pH value, initial rhodamine B concentration, ultrasonic vibration frequency, output power and TiO_2 nanoparticles dosage were 500 r/min, 7, 20 mg/L, 40 kHz, 300 W and 500 mg/L respectively. Finally, degradation mechanism was discussed. The results indicate that ultrasound-assisted TiO_2 photocatalysis method is of great potential application value in removal of organic pollution and environmental purification.

1. Introduction

At present, with the development and progress of society, human beings are exerting more and more pressure on the ecological environment (Omran et al., 2016; Banerjee et al., 2016). A large number of toxic and harmful substances are produced in our daily life and production (GRIZZETTI et al., 2017). These substances are constantly circulating in the environment and continue to endanger the earth (YU et al., 2017). Among them, industrial wastewater is particularly harmful to the environment. Water is an indispensable substance for living organisms, and water pollution can cause great harm to the entire ecosystem and human health (LI et al., 2016; YAN et al., 2015). Therefore, it makes sense to find effective ways to treat pollutants in water (ZHANG et al., 2017). So far, the methods commonly utilized in everyday society to treat organic pollutants in wastewater are chemical reduction and oxidation, activated carbon adsorption and microbial treatment methods (TARAN et al., 2018). Although these methods have achieved certain results in the treatment of wastewater, there are some defects, such as incomplete removal of pollutants, low efficiency and energy consumption (DOMÍNGUEZ et al., 2014; Wang, 2020).

Rhodamine B(RhB) is a widely used cationic basic dye, which belongs to anthraquinone (Wang, 2018a). The wastewater produced by this dye is characterized by high chromaticity, difficult biochemical degradation and high concentration of organic pollutants (Wang, 2018b). Traditional adsorption techniques to degrade RhB produce secondary pollution, while biochemical techniques make it difficult to degrade chemically stable RhB (YAO et al., 2018).

TiO_2-based photocatalysis, as a green and efficient water treatment technology, can degrade organic pollutants into small molecules, such as CO_2 and H_2O. In the field of wastewater treatment, it has a broad application prospect (CHOI et al., 2018; Xu and Bao, 2020). However, at present, TiO_2 photocatalysts still have problems such as low reaction efficiency, low solar energy utilization and unsatisfactory treatment of high concentration wastewater, therefore, they need to be combined with other methods to improve the catalytic efficiency (HE et al., 2016; PANDA and MANICKAM, 2017).

With the continuous research in the field of ultrasound, its ability to catalyze the degradation of organic matter has been used to degrade wastewater (ZHANG et al., 2014). Under the action of ultrasonic waves, a large number of cavitation bubbles are formed in the liquid (QIU et al., 2018). The cavitation bubbles undergo oscillation, growth, contraction and collapse in a very short period of time, forming a high temperature and high-pressure hot spot around the cavitation nucleus at a

* Corresponding author.
E-mail addresses: hailingma@yeah.net, CISY_EDUCN@126.COM (H. Ma).
[1] These authors contribute equally to this article.

https://doi.org/10.1016/j.jclepro.2021.127758
Received 27 January 2021; Received in revised form 30 April 2021; Accepted 29 May 2021
Available online 9 June 2021

Notation

DR%	The degradation rate
C0	The initial concentration of Rhodamine B (mg/l)
Ct	Concentration of Rhodamine B at the time t (mg/l)
e	Negative electron
h^+	Electron hole

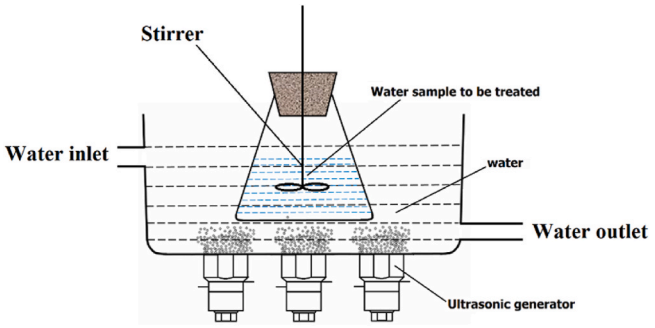

Fig. 1. Experimental setup.

temperature of 1900–5000 K and a pressure of 50 MPa, accompanied by strong shock waves and micro-jets (Wang et al., 2019). Thus, it oxidizes and decomposes the volatile organic compounds entering the cavitation bubble (SANTOS et al., 2012).

As a wide-band gap semiconductor, TiO_2 has been widely used in many research fields, such as photocatalysis, chemical sensors, solar cells and lithium-ion batteries, due to its high catalytic activity, biocompatibility, antibacterial properties and UV absorption (Xu et al., 2021a; SONG et al., 2018). Relevant studies have shown that the huge instantaneous energy released by ultrasonic cavitation can meet the needs of TiO_2 valence band electron transition (TABASIDEH et al., 2017), thus producing a catalytic action similar to photocatalysis (YUAN et al., 2018). Therefore, it is of great significance to select TiO_2 nanoparticles as catalyst to combine with ultrasound for related degradation experiments (Yan et al., 2010). The preferential nucleation and catalytic activity on the surface of TiO_2 solid particles can be used for catalytic degradation of organic pollutants (Chong et al., 2010). The fractured cavitation bubble will reach the surface of the nanoparticles under the light radiation to initiate the catalytic properties of TiO_2(Momeni et al., 2015). The combination energy of ultrasonic and TiO_2 nanoparticles can overcome the shortcoming that the light is not permeable enough in liquid and easily blocked by catalyst particles, so organic pollutants can be better degraded (Xu et al., 2020a, 2021b). In addition, the hydroxyl radical generated by ultrasonic cavitation and the hydroxyl radical generated by TiO_2 catalysis also have a synergistic effect (Qian et al., 2018). It can mineralize and degrade organic pollutants more effectively (Qian et al., 2019). Meanwhile, TiO_2 nanoparticles can be modified to further increase the degradation efficiency (Xu et al., 2020b).

In this paper, catalytic degradation of Rhodamine B form water by ultrasound-assisted TiO_2 photocatalysis is investigated. Firstly, the experimental materials and equipment are given, and the experimental procedures are introduced; Secondly, the influence of ultrasonic factors on the degradation of rhodamine B was discussed; Thirdly, the effects of initial conditions on the ultrasonic catalytic degradation of rhodamine B were studied; Finally, the reaction mechanism is analyzed. The optimal degradation conditions were obtained, and the mechanism of degradation of Rhodamine B in wastewater by ultrasound-assisted TiO_2 photocatalysis is given. The results indicate that ultrasound-assisted TiO_2 photocatalysis method is of great potential application value in removal of organic pollution and environmental purification. The purpose of this paper is to prove that the combination method of ultrasound, TiO_2 nanoparticles and mechanical stirring is of great potential application value in removal of organic pollution and environmental purification.

2. Experimental equipment

The experimental equipment for ultrasonic degradation research is shown in Fig. 1, which is mainly composed of ultrasonic source system, circulating water system and reaction system. The ultrasonic source system is composed of ultrasonic transducer and other parts of the cleaning machine. The circulating water system controls the temperature of the whole system by using the real-time temperature display of the ultrasonic cleaning machine. The reaction system consists of three parts: the reaction vessel, the reaction solution and the stirring rod. The stirring rod is connected with an electric agitator to control and record the speed of mechanical stirring in real time.

3. Experimental materials and instruments

All the chemicals in the study experiment were analytical grade. Tetrabutyl titanate ($C_{16}H_{36}O_4Ti$) and Ethanol (CH_3CH_2OH) were taken as a titanium source and the reaction solution respectively. Rhodamine B ($C_{28}H_{31}N_2O_3Cl$) was used as the dye to simulate organic pollutants.

The specific steps are as follows: TiO_2 nanoparticles were prepared by muffle furnace (XH2L-10, Zhengzhou Xinhan Instrument Equipment Co., Ltd), constant temperature magnetic stirrer (85-2B, Shandong Boke Regenerative Medicine Co. Ltd) and vacuum drying oven (YZG-600, Changzhou Shengerling Drying Pelletizing Equipment Co., Ltd); Ultrasonic cleaning machine (ADS-1720Q, Foshan Andixin Ultrasonic Cleaning Equipment Co., Ltd) was used as the radiation source for the ultrasonic catalytic degradation experiment; Mechanical stirring and speed measurement are carried out with precision electric stirrer (JJ-1A, Jintan City Chengdong Hongye Experimental Instrument Factory); A high-speed centrifuge (JIDI-20D, Guangzhou Jidi Instrument Co., Ltd) is used to separate the nanoparticles from the solution; The degradation effect of Rhodamine B, a dye simulating organic pollutants, was measured by ultraviolet spectrophotometer (722S, Jining Yuze Industrial Technology Co., Ltd).

4. Experimental steps of ultrasound-assisted photocatalytic degradation

All experiments were conducted at a constant temperature (24 °C). Rhodamine B was prepared into five kinds of solutions with concentrations of 5 mg/L, 10 mg/L, 15 mg/L, 20 mg/L and 25 mg/L, respectively. Then pure TiO_2 nanoparticles prepared at the concentrations of 250 mg/L, 500 mg/L, 750 mg/L, 1000 mg/L and 1250 mg/L were added to them respectively. The reaction mixture was stirred continuously for 1 h to reach the adsorption-desorption equilibrium level. It should be emphasized that the whole experimental reaction process was carried out under supersonic - mechanical agitation. A small amount of solution was extracted from the reaction system at certain intervals of reaction time, and then all the floating pure TiO_2 nanoparticles were removed using a high-speed centrifuge. The absorbance values of the separated clarified reaction solution were measured by UV–vis spectrophotometer. The absorbance value of rhodamine B was measured at 554 nm and the concentration of the reaction solution was calculated from the standard curve of rhodamine B solution. The degradation rates are defined as (Jaroo et al., 2019):

$$DR\% = \frac{C_0 - C_t}{C_0} X100 \quad (1)$$

where Co is the initial concentration of Rhodamine B (mg/l) and Ct is concentration of Rhodamine B at the time t (mg/l).

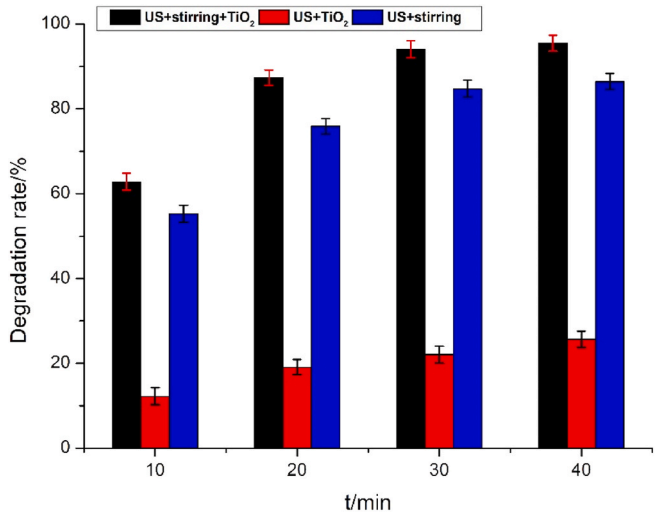

Fig. 2. Effect of catalyst dosage and mechanical agitation on degradation rate under ultrasonic treatment.

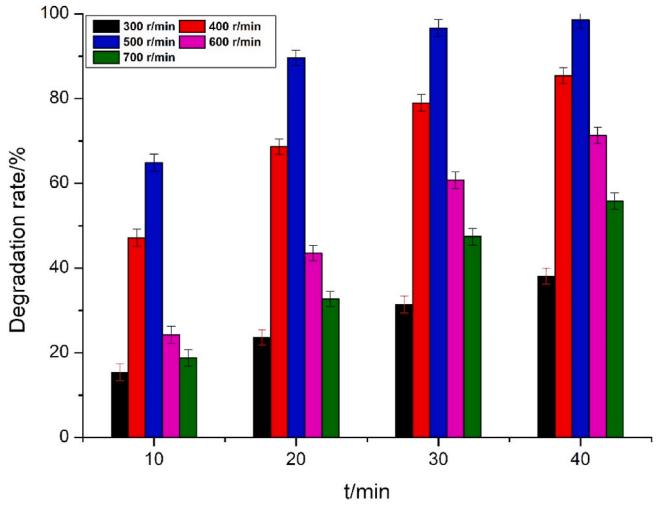

Fig. 3. Effect of mechanical rotational speed on degradation rate.

The maximum absorption wavelength of Rodamine B solution is 554 nm. As the degradation process progressed, the peak absorption wavelength of rhodamine B basically remained unchanged, but its absorbance gradually decreased, indicating that rhodamine B had been gradually degraded under the combined action of TiO_2 photocatalysis and ultrasound (Borowski, 2020).

5. Factors influencing the ultrasound-assisted TiO_2 photocatalytic degradation for rhodamine B

The effects of various factors, such as the amount of catalyst, the speed of mechanical stirring, the frequency of ultrasonic vibration, the ultrasonic output power, the initial pH value of the reaction solution, the initial concentration of Rhodamine B, the introduced air, and physical adsorption, etc., on the degradation of Rhodamine B in wastewater were studied. The reaction mixture solution with an initial capacity of 250 mL was degraded, and 10 ml was absorbed from the reaction solution each time for high-speed centrifugal treatment. Then the absorbance of the clarified solution was measured (Mirra et al., 2020).

5.1. Effect of catalyst dosage and mechanical agitation on degradation rate under ultrasonic treatment

Under certain experimental reaction conditions, Rhodamine B solution with 20 mg/l concentration was degraded and the solution was absorbed from the reaction system every 10 min. The experimental conditions are as follows: US + stirring, US + TiO_2, and US + stirring + TiO_2.

It can be seen from Fig. 2 that under the three conditions, the degradation effect is increasing with time. When the degradation is carried out to 40 min, the degradation rates of the three method reach 95.48%, 25.66%, 86.44% respectively. It was found that the mechanical stirring had a great influence on the degradation rate, and the addition of nanoparticles could promote the degradation reaction efficiency in the reaction system. As the reaction system is done in the ultrasonic cleaner, the cavitation bubble may be more difficult to reach the critical value of rupture. This is consistent with the phenomena observed during the experiments, such as the continuous growth of bubbles in the solution. They keep bouncing up and down in the solution under the action of ultrasonic waves to reach the size visible to the naked eye, but it is difficult to rupture for a long period of time. However, the addition of mechanical stirring accelerates the rate of bubble rupture by causing the bubbles to break once they reach a -determined size. At the same time, it also accelerates the intensity of the reaction between substances. The increase in the number of hydroxyl radicals generated in the solution under the high temperature and pressure conditions produced by the bubble rupture led to an increase in the degradation efficiency of organic dyes. Meanwhile, the addition of solid nanoparticles provides a preferred nucleation location for cavitation bubbles. The non-homogeneous phase is easier to nucleate than the homogeneous phase and will generate more cavitation bubbles to accelerate the degradation reaction.

5.2. Effect of mechanical rotational speed on degradation rate

The mechanical speed of the ultrasonic cleaner was set to 300 r/min, 400 r/min, 500 r/min, 600 r/min and 700 r/min, respectively. Other experimental conditions were as above, and the effect of different mechanical speeds on the degradation of rhodamine B at the initial reaction concentration of 20 mg/L was investigated. It is important to emphasize that the mixed solution was drawn from the reaction system every 10 min. The effect of mechanical rotational speed on degradation rate is shown in Fig. 3.

As can be seen from Fig. 3, at different mechanical rotational speeds, the degradation efficiency increases with the increase of ultrasonic treatment time, when US catalysis reaches 40 min, the degradation rates at different mechanical rotational speeds were 38.08% (300 r/min), 85.41% (400 r/min), 98.60% (500 r/min), 71.33% (600 r/min) and 55.80% (700 r/min) respectively. It can be found that the degradation efficiency first increases with the increase of revolutions per minute and reaches the best degradation effect at 500 r/min, then the degradation effect starts to decrease with the increase of mechanical speed. It can also be seen that the rotational speed has a significant effect on the degradation rate.

In the solid nanoparticle reaction system, the cavitation bubbles did not collapse completely and rapidly at low revolutions per minute, while the cavitation bubbles did not increase to a certain size and rupture at high revolutions per minute, which led to a decrease in the efficiency of hydroxyl radical production and thus degradation efficiency. Besides, in the nanoparticle reaction system, either too low or too high rotational speed leads to less efficient production of hydroxyl radicals and thus the degradation efficiency is reduced (Buaisha et al., 2020).

5.3. Ultrasonic frequency

The ultrasonic vibration frequencies were set to 25 kHz, 40 kHz, 60 kHz and 80 kHz, respectively, and the other experimental conditions were the same as above. The effect of ultrasonic frequency on the

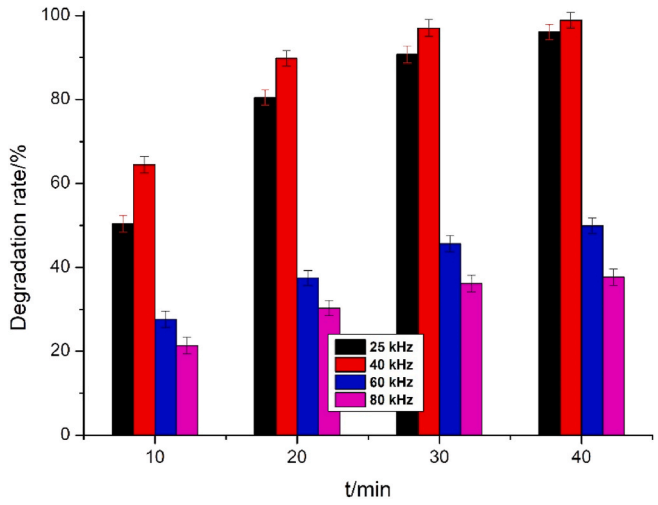

Fig. 4. Effect of US frequency on degradation of Rhodamine B.

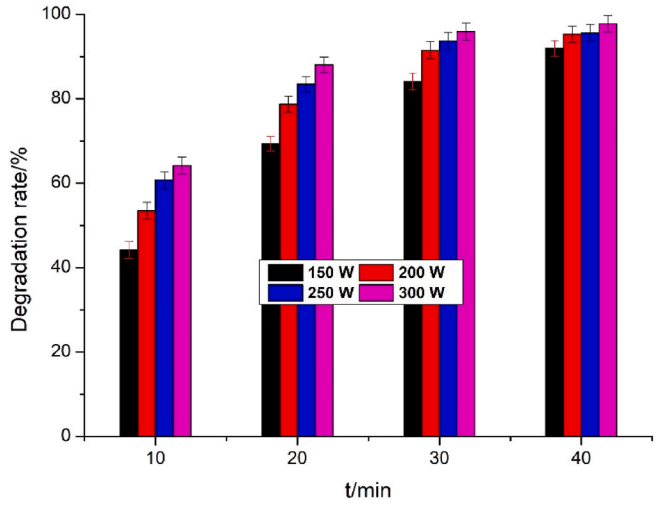

Fig. 5. Effect of US power on degradation of Rhodamine B.

degradation of rhodamine B at the initial reaction concentration of 20 mg/L was investigated. Similarly, the mixed solution is drawn from the reaction system every 10 min. The effect of ultrasonic frequency on degradation rate is shown in Fig. 4.

As can be seen from Fig. 4, under different ultrasonic vibration frequencies, the overall trend of ultrasonic degradation efficiency gradually increases with the increase of ultrasonic irradiation time. Firstly, the degradation effect at 40 kHz was significantly better than that at 25 kHz and 40 kHz in the first 30 min. At 30 min, the degradation rates of the two were 90.74% and 97.05%, respectively. However, with the extension of time, there was no significant difference in the degradation efficiency at the two frequencies, and the degradation rates were 96.04% and 98.88%, respectively. This may be because the overall degradation efficiency of the reaction has reached a relatively high level, and the concentration of pollutants in the reaction system has been relatively reduced, but there is no significant difference in the degradation effect. Secondly, at 60 kHz and 80 kHz, there is a continuous great change in the degradation efficiency with the continuation of the reaction time. At 30 min, the degradation efficiency at two frequencies 45.65% and 36.13%, respectively; At 40 min, the difference of the two degradation efficiency became greater, and the degradation efficiency was 49.94% and 37.69%, respectively. Finally, it was found that low-frequency ultrasonic radiation could achieved a higher degradation rate. Since the ultrasonic effect at 40 kHz in a short period of time had a greater

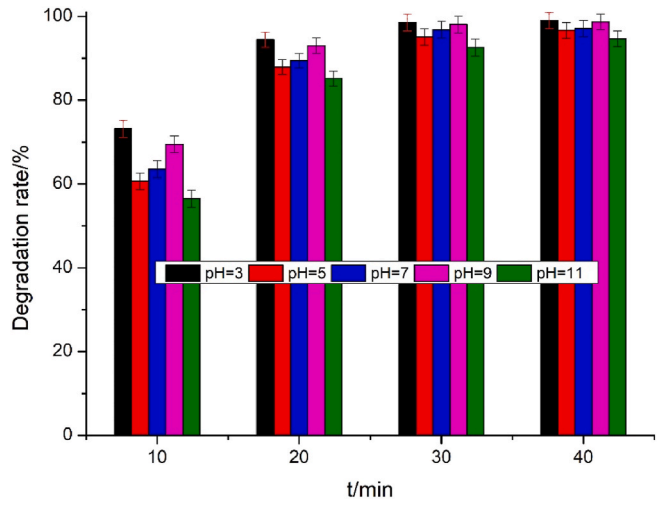

Fig. 6. Effect of initial pH value on US degradation of Rhodamine B.

degradation effect, the optimal frequency selection should be set to 40 kHz. The possible reason for this phenomenon is that relatively low-frequency ultrasound is more likely to nucleate on the surface of solid nanoparticles under the action of ultrasound, thus generating more cavitation bubbles and promoting the degradation reaction.

5.4. Ultrasonic power

Ultrasonic powers are set to 150 W, 200W, 250 W and 300 W respectively, and the other experimental conditions were the same as above. The effect of ultrasonic power on the degradation of rhodamine B at the initial reaction concentration of 20 mg/L was investigated. Similarly, the mixed solution is drawn from the reaction system every 10 min. The effect of ultrasonic power on degradation rate is shown in Fig. 5.

As can be seen from Fig. 5, at different US power, the degradation efficiency increases over time, at 40 min, the maximum degradation effect is achieved. At 40 min, the degradation rates under different ultrasonic power were 91.89% (150 W), 95.28 (200 W), 95.63% (250 W) and 97.77% (300 W) respectively. It can be found that the degradation efficiency increases with the increase of ultrasonic power. When the maximum output power is reached, the ultrasonic degradation effect reaches the maximum. The possible reasons are as follows: firstly, high output power facilitates the cavitation bubbles after nucleation to be easy to separate from the surface of nanoparticles; secondly, due to the increase of power, the energy transferred into the reaction solution within a certain time increases, which accelerates the growth and collapse period of cavitation bubbles and thus leads to the improvement of degradation efficiency.

In addition, to achieve rapid ultrasonic degradation rates, degradation by ultrasonic alone usually requires a large amount of electrical energy because there is a large amount of energy lost in heat consumption, which hinders the wide application of ultrasonic degradation in practical water treatment. The combination method of ultrasound, TiO_2 nanoparticles and mechanical stirring can well reduce the consumption of electric energy and accelerate the degradation process of rhodamine B.

5.5. Initial pH

The initial pH values of the reaction solution are set to 3, 5, 7, 9 and 11 respectively, and the other experimental conditions were the same as above. The effect of initial pH on the degradation of rhodamine B at the initial reaction concentration of 20 mg/L was investigated. Similarly, the mixed solution is drawn from the reaction system every 10 min. The

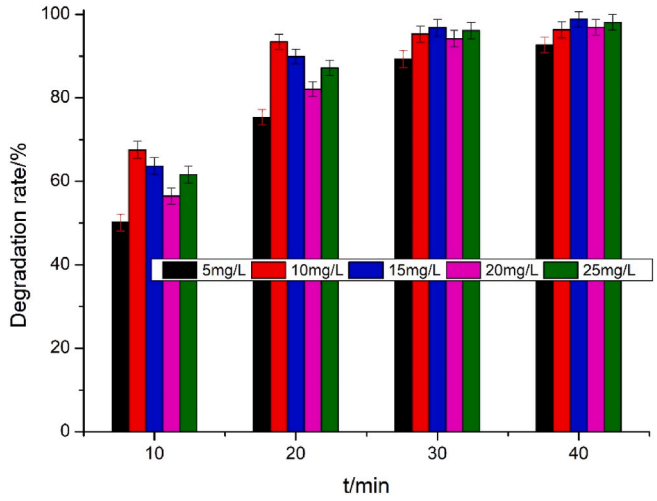

Fig. 7. Effect of initial concentration of Rhodamine B on degradation.

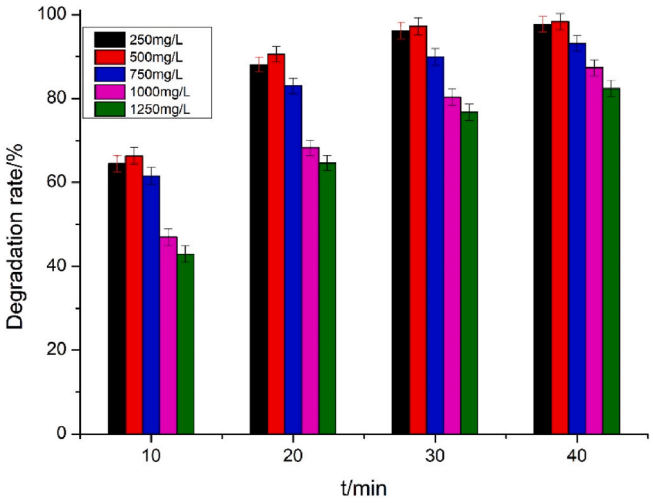

Fig. 8. Effect of TiO_2 addition on US degradation of Rhodamine B.

effect of initial pH on degradation rate is shown in Fig. 6.

It can be seen from the figure that, in a relatively short period of time, the degradation efficiency of rhodamine B solution with acidic pH was slightly higher than that of rhodamine B solution with alkaline pH, but the overall degradation effect difference was not obvious. At 40 min, the degradation rates at different pH values were 99.8% (pH = 3), 99.6% (pH = 5), 98.6% (pH = 7), 97.8% (pH = 9) and 96.9% (pH = 11) respectively. The results showed that different pH values had no obvious effect on the ultrasonic degradation efficiency of rhodamine B, indicating that rhodamine B was relatively stable under different pH values. Besides, both high and low pH values are unfavorable for the degradation of Rhodamine B. This is because Rhodamine B is an amphoteric compound, i.e., it has a positive charge at low pH and a negative charge at high pH. Excessive positive and negative charges are not conducive to its adsorption by TiO_2. Only when the system is close to neutral is it favorable for rhodamine B, which is thus destroyed by the radical on the surface of TiO_2 and accelerates its degradation. After comprehensive analysis, 7 was determined as the best degradation pH value.

5.6. Initial concentration of rhodamine B

The initial concentrations of Rhodamine B are set to 5 mg/l, 10 mg/l, 15 mg/l, 20 mg/l and 25 mg/l respectively, and the other experimental conditions were the same as above. The effect of initial concentrations of Rhodamine B on the degradation of rhodamine B was investigated. Similarly, the mixed solution is drawn from the reaction system every 10 min. The effect of initial concentration on degradation rate is shown in Fig. 7.

According to Fig. 7, as the concentration gradient increases, the degradation efficiency increases first and then decreased. At 20 min, the degradation rates at different initial concentrations of Rhodamine B were 75.39% (5 mg/l), 93.44% (10 mg/l), 89.87% (15 mg/l), 82.14% (20 mg/l) and 87.17% (25 mg/l) respectively. In the reaction system, the optimum initial degradation concentration of Rhodamine B is 20 mg/l. With the increase of the initial concentration, the content of organic dyes at the gas-liquid interface of cavitation bubble increases, and hydroxyl radical produced by cavitation bubble rupture has an effective erosion effect on organic dyes, making organic dyes degradation. At the same time, when organic dyes reach a certain concentration, they will adhere to the surface of solid nanoparticles, affecting the nucleation of cavitation bubbles, thus reducing the degradation efficiency. Therefore, it is necessary to select the appropriate initial concentration in the experimental system to study and explore the ultrasonic catalytic degradation reaction.

It was further found that, however, when the concentration continued to increase, the degradation rate started to decrease instead. This may be due to the fact that at low initial concentrations, Rhodamine B is adsorbed on the TiO_2 surface and destroyed by the radicals generated on its surface. With the further increase of the concentration, the surface adsorption capacity of TiO_2 reached saturation, and Rhodamine B was relatively excessive. In addition, most of the TiO_2 surface was covered by Rhodamine B, which also affected the generation of radicals, thus leading to a decrease in the degradation rate. A similar situation occurred for the system without TiO_2 catalyst, but for different reasons. The degradation ability of ultrasonic alone is limited, and excessive Rhodamine B naturally reduces the degradation rate.

5.7. The amount of TiO_2 addition

Amounts of TiO_2 nanoparticles added are set to 250 mg/l, 500 mg/l, 750 mg/l, 1000 mg/l and 1250 mg/l respectively. The effect of TiO_2 addition on the degradation of rhodamine B with the initial reaction concentration of 20 mg/L was investigated. Similarly, the other experimental conditions were the same as above. The effect of initial concentration on degradation rate is shown in Fig. 8.

As can be seen from Fig. 8, when 250 mg/l and 500 mg/l TiO_2 is added, compared with other addition, the degradation efficiency is higher. At 20 min, the degradation efficiency is 89.52% and 90.63% respectively. At 40 min, the degradation efficiency is 98.83% and 98.92%, respectively; At 20 min, the degradation rates corresponding to 750 mg/l, 1000 mg/l and 1250 mg/l were 84.14%, 69.52% and 65.24% respectively; At 40 min, the degradation rates corresponding to 750 mg/l, 1000 mg/l and 1250 mg/l were 93.82%, 88.14% and 83.26% respectively. It can be found that with the increase of nanoparticles, the degradation effect of US catalysis increases first and then decreases. The results show that when the catalytic time is 40 min and the concentration of nanoparticles is 500 mg/L, the best ultrasonic degradation effect is obtained. The reasons may be as follows: First, with the increase of nanoparticle concentration, the nucleation location of cavitation bubbles increases, leading to the increase of degradation efficiency. Secondly, when the concentration of nanoparticles increases again, the concentration of nanoparticles in the solution reaches the saturation value, and the interaction between the particles leads to the relative decrease of heterogeneous nucleation sites. Besides, When the addition amount of TiO_2 increased, the ·OH radical generated in the solution also increased under the action of ultrasonic wave. However, when the TiO_2 incorporation amount exceeded a certain value, the utilization of ultrasonic waves decreased due to mutual shielding between catalysts, and thus the degradation rate decreased (Kibaara et al., 2020).

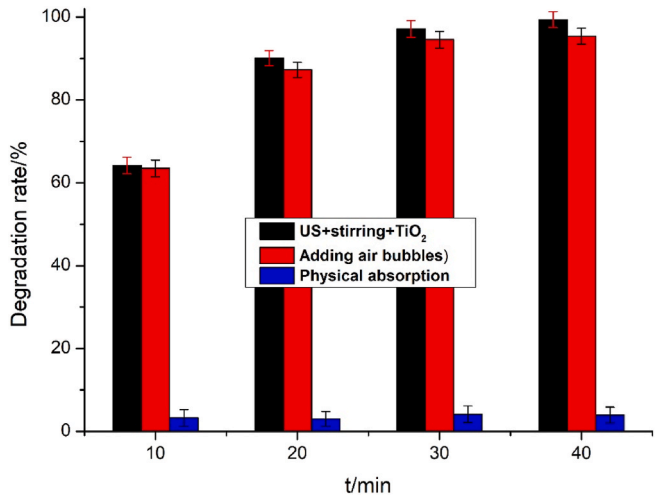

Fig. 9. Effects of bubble addition and physical adsorption on US degradation of Rhodamine B.

5.8. Effects of bubble addition and physical adsorption on degradation rate

Add air and nano-absorbent particles to the reaction solution to investigate their effect on the degradation of Rhodamine B solution with the initial reaction concentration of 20 mg/L. Similarly, the other experimental conditions were the same as above. The results are shown in Fig. 9.

It can be seen from Fig. 9 that the physical adsorption of nanoparticles has no significant effect on the degradation efficiency under the same mechanical stirring intensity. This is consistent with previous studies, most adsorbed organic dyes undergo desorption within 10 min under US-mechanical stirring. The degradation efficiency is 90.11% and 87.27% at 20 min and 98.39% and 95.38% at 40 min respectively under the experimental conditions without adding air and adding air. Studies have shown that the degradation rate of rhodamine B was 91.7% using ultrasound-assisted micro spherical $Bi_2O_2CO_3$(Dong-dong et al., 2019), and 94.6% by sodium persulfate activated with Fe_3O_4-modified hydrochar (ZHANG et al., 2020). By comparison, it can be proved that the ultrasound-assisted TiO_2 photocatalysis degradation for Rhodamine B is more effective.

It can be found that excessive bubbles can slightly reduce the degradation effect. The possible reason is that, first, the addition of bubbles leads to changes in the original reaction system, resulting in a decrease in the number of hydroxyl radicals. Secondly, the experimental results show that stirring accelerates the collapse of ultrasonic cavitation bubbles and has a significant effect on the degradation reaction, while the addition of air bubbles affects its own cavitation bubble nucleation.

6. Degradation mechanism

Degradation mechanism of Rhodamine B in wastewater with the combination of ultrasound, TiO_2 nanoparticles and mechanical stirring is shown in Fig. 10. Firstly, cavitation bubbles undergo nucleation process. The surface and volume solution of nano solid particles are nucleation, and nucleation is relatively easy on the surface of solid particles. Secondly, cavitation bubbles grow continuously under ultrasonic action. Finally, cavitation bubbles reach a certain size and collapse under the action of ultrasound. At the same time, in a very short time, ultrasonic radiation forms "sonic luminescence" (SL) and generates high temperature, which causes hydrothermal decomposition to generate hydroxyl radicals (2). The light and heat generated by ultrasonic cavitation can excite nanoparticles, so that electron-hole (e^- is Negative electron, h^+ is Electron hole) pairs are continuously formed. Then, a series of reactions take place to produce some active substances, such as O_2, H_2O_2 and OH (3–5). These powerful oxidants can attack organic dyes and degrade them.

$$H_2O \rightarrow H\cdot + \cdot OH. \quad (2)$$

$$O_2 + e^- \rightarrow .O_2^- \quad (3)$$

$$O_2^- + H_2O \rightarrow H_2O_2. \quad (4)$$

$$H_2O_2 + \cdot O_2^- \rightarrow \cdot OH + OH^- + O_2 \quad (5)$$

7. Conclusion

In this paper, degradation of Rhodamine B in wastewater by ultrasound-assisted TiO_2 photocatalysis was investigated. The main conclusions are as follows:

(1) In the reaction system of nanoparticles, too low or too high rotational speed will lead to the reduction of the generation efficiency of hydroxyl radical, thus reducing the degradation efficiency.

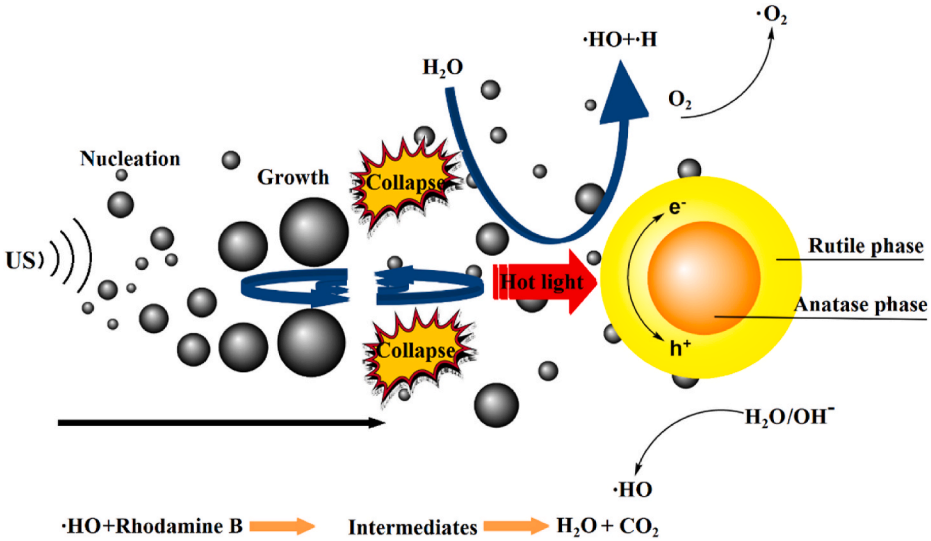

Fig. 10. Degradation process of Rhodamine B by ultrasound-assisted TiO_2 photocatalysis.

(2) With the increase of ultrasonic irradiation time, the degradation efficiency showed a trend of gradual increase. High degradation rates were obtained with low frequency ultrasound radiation.
(3) The degradation efficiency increased continuously with time at different ultrasound powers. With the increase of ultrasonic power, the degradation efficiency showed an increasing trend. When the ultrasonic power reached the maximum output power of the experimental reaction system, the ultrasonic degradation effect reached the maximum.
(4) Different pH values had no significant effect on the degradation efficiency of rhodamine B by ultrasound-assisted photocatalysis.
(5) With the increase of the concentration gradient of the reaction solution, the degradation efficiency showed a trend of increasing first and then decreasing.
(6) The ultrasound-assisted catalytic degradation efficiency showed a trend of increasing and then decreasing with the increase of nanoparticle addition.

Author statement

First author: Dong Xu
College of Geomatics and Municipal Engineering, Zhejiang University of Water Resources and Electric Power, Hangzhou 310018, China
Email: xud@zjweu.edu.cn
ORCID: 0000-0002-9111-1245
Corresponding author: Hailing Ma Institute of Mechanics, Chinese Academy of Sciences, Beijing, 100190, PR China
Email: hailingma@yeah.net
ORCID: 0000-0001-5650-3713

Declaration of competing interest

The authors declare that they have no known competing financial interests or personal relationships that could have appeared to influence the work reported in this paper.

References

Banerjee, S., Sharma, G.C., Gautam, R.K., 2016. Removal of Malachite Green, a hazardous dye from aqueous solutions using Avena sativa (oat) hull as a potential adsorbent[J]. J. Mol. Liq. 213, 162–172.
Borowski, Piotr F., 2020. New technologies and innovative solutions in the development. High Tech. Innovat. J. 1 (No. 2), 39–58. https://doi.org/10.28991/HIJ-2020-01-02-01. June.
Buaisha, Magdi, Balku, Saziye, Oz, Şeniz, 2020. Heavy metal removal investigation in conventional activated sludge systems. Civil Engineering Journal 6 (No. 3), 470–477. https://doi.org/10.28991/cej-2020-03091484. March.
Choi, J., Cui, M., Lee, Y., et al., 2018. Synthesis, characterization and sonocatalytic applications of nano-structured carbon based TiO_2 catalysts[J]. Ultrason. Sonochem. 43, 193–200.
Chong, M.N., Jin, B., Chow, C.W.K., et al., 2010. Recent developments in photocatalytic water treatment technology: a review[J]. Water Res. 44 (10), 2997–3027.
Domínguez, C.M., Quintanilla, A., Casas, J.A., 2014. Kinetics of wet peroxide oxidation of phenol with a gold/activated carbon catalyst[J]. Chem. Eng. J. 253, 486–492.
Dong-dong, D.U., Cheng-hui, W.A.N.G., Gang-qiang, Z.H.U., Deng, Qing-song, Yan-peng, L.I., Sun, Yong-jie, 2019. Research on sonocatalytic degradation of Rhodamine B by $Bi_2O_2CO_3$ particles under ultrasonic irradiation. Tech. Acoust. 38 (No.3), 301–306. Jun.
Grizzetti, B., Pistocchi, A., Liquete, C., 2017. Human pressures and ecological status of European rivers[J]. Sci. Rep. 7 (1), 205.
He, L.L., Liu, X.P., Wang, Y.X., et al., 2016. Sonochemical degradation of methyl orange in the presence of Bi_2WO_6: effect of operating parameters and the generated reactive oxygen species[J]. Ultrason. Sonochem. 33, 90–98.
Jaroo, Suhad Shamil, Jumaah, Ghufran F., Abbas, Talib R., 2019. Photosynthetic microbial desalination cell to treat oily wastewater using microalgae chlorella vulgaris. Civil Engineering Journal 5 (12), 2686–2699. December.
Kibaara, Samuel Kariuki, Murage, D.K., Musau, P., Saulo, M.J., 2020. Comparative analysis of implementation of solar PV systems using the advanced SPECA modelling tool and HOMER software: Kenyan scenario. High Tech and Innovation Journal 1 (No. 1), 8–20. https://doi.org/10.28991/HIJ-2020-01-01-02. March.
Li, X., Yin, P., Zhao, L., 2016. Phthalate esters in water and surface sediments of the Pearl River Estuary: distribution, ecological, and human health risks[J]. Environ. Sci. Pollut. Control Ser. 23 (19), 19341–19349.
Mirra, Renata, Ribarov, Christian, Valchev, Dobril, Ribarova, Irina, 2020. Towards energy efficient onsite wastewater treatment. Civil Engineering Journal 6 (No. 7), 1218–1226. https://doi.org/10.28991/cej-2020-03091542. July.
Momeni, M.M., Ghayeb, Y., Ghonchegi, Z., 2015. Fabrication and characterization of copper doped TiO_2 nanotube arrays by in situ electrochemical method as efficient visible-light photocatalyst[J]. Ceram. Int. 41 (7), 8735–8741.
Omran, A.R., Baiee, M.A., Juda, S.A., 2016. Removal of Congo red dye from aqueous solution using a new adsorbent surface developed from aquatic plant (Phragmites australis) [J]. International Journal of Chem Tech Research 9 (4), 334–342.
Panda, D., Manickam, S., 2017. Recent advancements in the sonophotocatalysis (SPC) and doped sonophotocatalysis (DSPC) for the treatment of recalcitrant hazardous organic water pollutants[J]. Ultrason. Sonochem. 36, 481–496.
Qian, X., Han, H., Chen, Y., et al., 2018. Sol-gel solvothermalroute to synthesize anatase/brookite/rutile TiO_2 nanocomposites with highly photocatalytic activity[J]. J. Sol. Gel Sci. Technol. 85 (2), 394–401.
Qian, R., Zong, H., Schneider, J., et al., 2019. Charge carrier trapping, recombination and transfer during TiO_2 photocatalysis: an overview[J]. Catal. Today 335, 78–90.
Qiu, P., Park, B., Choi, J., et al., 2018. A review on heterogeneous sonocatalyst for treatment of organic pollutants in aqueous phase based on catalytic mechanism[J]. Ultrason. Sonochem. 45, 29–49.
Santos, R.S., Faria, G.A., Giles, C., 2012. Iron insertion and hematite segregation on Fe-doped TiO_2 nanoparticles obtained from sol-gel and hydrothermal methods[J]. ACS Appl. Mater. Interfaces 4, 5555–5561.
Song, S.J., Hao, C.C., Zhang, X.G., et al., 2018. Sonocatalytic degradation of methyl orange in aqueous solution using Fe-doped TiO_2 nanoparticles under mechanical agitation[J]. Open Chemistry 16, 1283–1296.
Tabasideh, S., Maleki, A., Shahmoradi, B., 2017. Sonophotocatalytic degradation of diazinon in aqueous solution using iron-doped TiO_2 nanoparticles[J]. Separ. Purif. Technol. 189, 186–192.
Taran, O.P., Zagoruiko, A.N., Yashnik, S.A., 2018. Wet peroxide oxidation of phenol over carbon/zeolite catalysts, kinetics and diffusion study in batch and flow reactors[J]. J. Environ. Chem. Eng 6 (2), 2551–2560.
Wang, Zhenjun, 2018a. State-of-the-art on the development of ultrasonic equipment and key problems of ultrasonic oil production technique for EOR in China. Renew. Sustain. Energy Rev. 82 (Part 3), 2401–2407. February.
Wang, Zhenjun, 2018b. Research on removing reservoir core water sensitivity using the method of ultrasound-chemical agent for enhanced oil recovery. Ultrason. Sonochem. 42, 754–758. April.
Wang, Zhenjun, 2020. Advances in ultrasonic production units for enhanced oil recovery in China. Ultrason. Sonochem. 60, 104791. January.
Wang, H., Chen, H., Chen, W., et al., 2019. Vapor–liquid equilibrium study of LiBr+ H_2O and LiBr+ $CaCl_2$+ H_2O systems[J]. Frontiers in Chemistry 7, 0.3389/fchem.2019.00890.
Xu, X., Bao, T., 2020. Research on the removal of near-well blockage caused by asphaltene deposition using sonochemical method[J]. Ultrason. Sonochem. 64, 104918. https://doi.org/10.1016/j.ultsonch.2019.104918.
Xu, X., Yuan, Z., Wang, Y., 2020a. Multi-target tracking and detection based on hybrid filter algorithm[J]. IEEE Access 8, 209528–209536. https://doi.org/10.1109/ACCESS.2020.3024928.
Xu, X., Zhang, N., Zhou, Y., et al., 2020b. The effects of NaI, KBr, and KI salts on the vapor-liquid equilibrium of the H_2O+ CH_3OH system[J]. Frontiers in Chemistry 8. https://doi.org/10.3389/fchem.2020.00192.
Xu, X., Karami, B., Shahsavari, D., 2021a. Time-dependent behavior of porous curved nanobeam[J]. Int. J. Eng. Sci. 160, 103455. https://doi.org/10.1016/j.ijengsci.2021.103455.
Xu, X., Karami, B., Janghorban, M., 2021b. On the dynamics of nanoshells[J]. Int. J. Eng. Sci. 158, 103431. https://doi.org/10.1016/j.ijengsci.2020.103431.
Yan, S.C., Li, Z.S., Zou, Z.G., 2010. Photodegradation of rhodamine B and methyl orange over boron-doped g-C3N4 under visible light irradiation[J]. Langmuir 26 (6), 3894–3901.
Yan, Q., Zhang, Z., Zhang, Y., 2015. Hierarchical Fe_3O_4 core shell layered double hydroxide composites as magnetic adsorbents for anionic dye removal from wastewater[J]. Eur. J. Inorg. Chem. (25), 4182–4191, 2015.
Yao, Y., Sun, M.X., Yuan, X.J., 2018. One-step hydrothermal synthesis of N/Ti^{3+} co-doping multiphasic TiO_2/BiOBr rheteojunctions towards enhanced sonocatalytic performance[J]. Ultrason. Sonochem. 49, 69–78.
Yu, Y., Zhou, L., Zhou, W., 2017. Decoupling environmental pressure from economic growth on city level: the case study of Chongqing in China[J]. Ecol. Indicat. 75, 27–35.
Yuan, H., Tan, S., Du, W., 2018. Heterogeneous bubble nucleation model on heated surface based on free energy analysis[J]. Int. J. Heat Mass Tran. 122, 1198–1209.
Zhang, L., Belova, V., Wang, H., et al., 2014. Controlled cavitation at nano/microparticle surfaces[J]. Chem. Mater. 26 (7), 2244–2248.
Zhang, Y., Zheng, T.X., Hua, Y.B., 2017. Delta manganese dioxide nanosheets decorated magnesium wire for the degradation of methyl orange[J]. J. Colloid Interface Sci. 490, 226–232.
Zhang, Kai, Wei, Xiuli, Wang, Bing, Jiang, Tao, Liu, Ke, 2020. Degradation of Rhodamine B by sodium persulfate activated with Fe_3O_4 modified hydrochar. Chem. Ind. Eng. Prog. 39 (No.7), 2867–2874. https://doi.org/10.16085/j.issn.1000-6613.2019-1550.